Energy Management of Three-Dimensional Minimum-Time Intercept

Hendrikus G. Visser,* Henry J. Kelley,† and Eugene M. Cliff‡
Virginia Polytechnic Institute and State University, Blacksburg, Virginia

A real-time computer algorithm to control and optimize aircraft flight profiles is described and applied to a three-dimensional minimum-time intercept mission. The proposed scheme has roots in two well-known techniques: singular perturbations and neighboring-optimal guidance. Use of singular-perturbation ideas is made in terms of the assumed trajectory-family structure. A heading/energy family of prestored point-mass-model state-Euler solutions is used as the baseline in this scheme. The next step is to generate a near-optimal guidance law that will transfer the aircraft to the vicinity of this reference family. The control commands fed to the autopilot (bank angle and load factor) consist of the reference controls plus correction terms that are linear combinations of the altitude and path-angle deviations from reference values, weighted by a set of precalculated gains. In this respect, the proposed scheme resembles neighboring-optimal guidance. However, in contrast to the neighboring-optimal guidance scheme, the reference control and state variables as well as the feedback gains are stored as functions of energy and heading in the present approach. Some numerical results comparing open-loop optimal and approximate feedback solutions are presented.

Nomenclature

$C_{L_{max}}$ = maximum lift coefficient
C_{D_o} = zero-lift drag coefficient
D = drag
E = specific energy
g = acceleration due to gravity
h = altitude
K = efficiency parameter
M = Mach number
n = load factor
n_L = lift limit
n_{max} = structural limit
q = dynamic pressure
S = wing area
t = time
T = thrust
V = velocity
W = weight
x = downrange
y = crossrange
γ = flight path angle
η = throttle setting
μ = bank angle
χ = heading

Superscripts

$( )^*$ = optimal value

Subscripts

$( )_D$ = value at dash point
$( )_f$ = final value
$( )_{fb}$ = feedback value
$( )_o$ = initial value
$( )_{ref}$ = reference value

Presented as Paper 85-1781-CP at the AIAA AFM Conference, Snowmass, CO; Aug. 19-21, 1986; received July 29, 1986; revision received Dec. 15, 1986.

*Graduate Student, Department of Aerospace and Ocean Engineering. Currently with Fokker B.V., Amsterdam, The Netherlands. Member AIAA.

†Professor, Department of Aerospace and Ocean Engineering. Fellow AIAA.

‡Professor, Department of Aerospace and Ocean Engineering. Member AIAA.

I. Introduction

DURING recent years the possibility of onboard real-time generation of guidance commands for aerial-combat missions has received considerable attention. In particular, several schemes for the minimum-time intercept of a target flying a completely defined maneuver have been developed. The solution to the two-point-boundary-value problem (TPBVP) associated with the intercept problem is typically found in open-loop form. However, onboard, real-time guidance generally requires the optimal control solution to be expressed in a feedback form. For this reason, approximate near-optimal closed-form feedback solutions are sought.

In this paper, an approach to onboard real-time calculations for a long-range air-to-air intercept mission in three dimensions is described. In this type of mission, the initial separation between the interceptor and the target is assumed relatively large, so that at least a portion of the interceptor's trajectory is flown at maximum velocity, i.e., a dash or cruise-dash arc is present. A guidance law is then developed, providing the interceptor a time-range-optimal turn-climb to the dash point on the flight envelope, fairing into a steady-state cruise-dash. The terminal maneuver following the turn-climb-dash sequence is not considered in this paper.

Several approaches to obtaining approximate closed-form feedback solutions to the target-intercept problem have been reported in recent studies. One approach of interest is based on singular-perturbation theory.[1,2,3] This approach takes advantage of the time-scale separation of the state variables by separating the dynamics into slow and fast modes (boundary-layer structure). Another approach to the intercept problem is by neighboring-optimal guidance technique.[4,5,6] In this approach, perturbation feedback control, i.e., control in the vicinity of a reference path, is considered. The resulting linear neighboring-optimal feedback guidance law controls the aircraft such as to follow a neighbor of the reference extremal. A third approach proceeds by flooding the state-space with extremals. A closed-loop controller is then synthesized from the open-loop results.[7,8]

The present approach, first sketched in Ref. 9, has roots in all three approaches just mentioned. The proposed scheme can properly be considered a singular-perturbation approach since it is based upon a similar hierarchical (multiple-boundary-layer) structure. It also resembles neighboring-

optimal guidance since it utilizes similar linear feedback laws to generate transients to the vicinity of a reference solution.

The present effort was encouraged by an earlier study in which the concept was applied to a climb-dash intercept mission in two dimensions.[10,11] The extension of the analysis from two to three dimensions is far from trivial. Essential points of difficulty include the substantially more involved numerical resolution of the TPBVP in the case of the three-dimensional problem and the identification of an appropriate hierarchial family structure.

II. Problem Statement

Equations of Motion

The equations of motion for a point-mass model of an aircraft can be written as

$$\dot{x} = V\cos\gamma\cos\chi \tag{1a}$$

$$\dot{y} = V\cos\gamma\sin\chi \tag{1b}$$

$$\dot{h} = V\sin\gamma \tag{1c}$$

$$\dot{E} = (V/W)[T-D] \tag{1d}$$

$$\dot{\gamma} = (g/V)[n\cos\mu - \cos\gamma] \tag{1e}$$

$$\dot{\chi} = (g/V)[n\sin\mu/\cos\gamma] \tag{1f}$$

where

$$V = [2g(E-h)]^{1/2} \tag{2}$$

is to be regarded as eliminated in favor of E and h. These equations embody the assumptions of a constant-weight vehicle, with thrust directed along the flight path and a flat nonrotating Earth. The equations of motion are written here in a fixed coordinate frame that has its origin at the interceptor's final position and its x axis aligned with the projection of the target's velocity vector on the horizontal plane. The heading is measured relative to the x axis. The target is assumed to be traveling on a constant course. The control variables in these equations are n, μ, and η.

Aerodynamic and Propulsive Force Models

The aerodynamic and propulsive forces are assumed to have the following form:

$$T = \eta T_{\max}(M,h) \tag{3}$$

$$D = D_o + n^2 D_i \tag{4}$$

where D_o is the zero-lift drag:

$$D_o = qSC_{D_o}(M) \tag{5}$$

and D_i is the induced drag in level flight ($n=1$):

$$D_i = K(M)W^2/qS \tag{6}$$

The following constraints on the control variables are specified:

$$0 \le \eta \le 1 \tag{7}$$

$$n \le n_{\max} \quad \text{(structural limit)} \tag{8}$$

$$n \le n_L = (qS/W)C_{L_{\max}} \quad \text{(lift limit)} \tag{9}$$

In the numerical examples, a realistic aircraft model, representative of a high-performance fighter, is used.[11]

Optimal-Control Formulation

The optimal-control problem is to determine the controls η^*, n^*, and μ^* such that, starting from the initial conditions

$$x(t_o)=x_o \quad h(t_o)=h_o \quad E(t_o)=E_o \tag{10a}$$

$$\gamma(t_o)=\gamma_o \quad \chi(t_o)=\chi_o \tag{10b}$$

the interceptor reaches the final conditions (cruise-dash point)

$$x(t_f)=0 \quad y(t_f)=0 \quad h(t_f)=h_D \tag{11a}$$

$$E(t_f)=E_D \quad \gamma(t_f)=0 \tag{11b}$$

in minimum time t_f (see Fig. 1). Note that the initial condition $y(t_o)$ and the final condition $\chi(t_f)$ are not prescribed. The reason for this will become apparent in subsequent analysis; it will be shown that using this formulation it is still possible to reach (asymptotically) the desired final heading $\chi(t_f)=0$.

The necessary conditions for optimality include the adjoint differential equations and transversality conditions

$$\dot{\lambda}_x = -\frac{\partial H}{\partial x} \tag{12a}$$

$$\dot{\lambda}_y = -\frac{\partial H}{\partial y}, \qquad \lambda_y(t_o)=0 \tag{12b}$$

$$\dot{\lambda}_h = -\frac{\partial H}{\partial h} \tag{12c}$$

$$\dot{\lambda}_E = -\frac{\partial H}{\partial E} \tag{12d}$$

$$\dot{\lambda}_\gamma = -\frac{\partial H}{\partial \gamma} \tag{12e}$$

$$\dot{\lambda}_\chi = -\frac{\partial H}{\partial \chi}, \qquad \lambda_\chi(t_f)=0 \tag{12f}$$

where H is the variational Hamiltonian, formed in the usual fashion. Since the system is autonomous and the final time t_f is not prescribed, there is a first integral (Mayer formulation)

$$H = -1 \tag{13}$$

Substantial simplification of the TPBVP is obtained by the analytic integration of the adjoint Eqs. (12a), (12b), and (12f). Using the transversality and final boundary conditions of Eq. (11a) results in the following expressions:[8,12]

$$\lambda_x = \text{constant} \tag{14a}$$

$$\lambda_y = 0 \tag{14b}$$

$$\lambda_\chi = \lambda_x y \tag{14c}$$

Going one step further, we can solve for λ_x in terms of the parameter $\lambda_\chi(t_f)$ by evaluating the first integral Eq. (13) at the steady-state final condition:

$$H\,|_{t=t_f}\, = \lambda_x V_D\cos\chi(t_f) = -1 \tag{15}$$

from which

$$\lambda_x = -1/[V_D\cos\chi(t_f)] \tag{16}$$

Assuming that an optimal control solution exists, the Minimum Principle can be used to express the optimal controls in terms of the state and adjoint variables. The TPBVP, determined by the system of state and adjoint equa-

tions with the appropriate boundary and transversality conditions, can be solved in open-loop form using some iterative numerical method. In the present effort, solutions are generated using a highly accurate Multiple-Shooting Algorithm (MSA).[13] Such solutions are presented in Sec. IV. Closed-form feedback solutions can be obtained if the intercept problem is treated in reduced-order (so-called "energy-state") approximation.

III. Energy-State Model

Singular Perturbation Approach

In the energy-state approximation, order-reduction is obtained by letting $\dot{h}$, $\dot{\gamma} \to 0$ in Eqs. (1c) and (1e), resulting in the algebraic constraints

$$\gamma = 0 \tag{17a}$$

$$n = 1/\cos\mu \tag{17b}$$

The remaining four state Eqs. (1) form the reduced-order system. The control variables in the energy-state model are η, μ, and h. Since the geometry of the intercept remains unchanged in the energy-state model, the expressions for the adjoints, Eqs. (14), are still valid. As a result, only one adjoint equation (governing λ_E) needs to be integrated in the energy-state model. If we consider symmetric flight only [$\mu(t) = 0$], no adjoint equations need to be integrated at all. In Ref. 14 it is shown that for the so-called energy-range climb (fixed-range, minimum-time energy-state solution),

$$\lambda_E = (V - V_D)/(V_D \dot{E}) \tag{18}$$

The right member of Eq. (18) is clearly singular when evaluated at the steady-state dash-point. In the energy-state approximation, the equilibrium point is reached only asymptotically.

Extremal-Field Solution

The particular form in which the energy-state model is written, allows a family of trajectories to be generated using an extremal-field approach. Starting from the terminal condition, the state-Euler equations are integrated backward in time, with an assumed value for the final heading. By varying the value of the final heading, the state-space is flooded with extremals. The final value of λ_E is obtained by evaluating Eq. (18) in the energy-range climb [it is recalled that $\lambda_\chi(t_f) = 0$ for the turn-climb trajectories].

General Features

In Fig. 2, several extremals in the (V,h)-space are sketched. In Fig. 3, some ground tracks are shown. If final heading is chosen identically zero, the (symmetric) energy-range climb path is obtained. The remaining members of the family (obtained by very small variations in the final heading) all reveal a similar behavior in retro-time: starting from the dash-point, the trajectories closely follow the energy-range path (in near-symmetric flight), but when the turn is initiated, altitude increases (possibly discontinuously) until the corner-velocity locus is reached. The trajectories will subsequently "ride" along the corner-velocity locus, with heading-to-go increasing in retro-time. This corner-velocity locus is a unique curve in the (V,h)-space characterized by a maximum instantaneous turn rate at each energy level.[1] The optimal throttle setting generally is full thrust; however, for large heading-to-go, throttle switching may occur.

It is observed that the turn-climb trajectories lie almost entirely within a corridor formed by the corner-velocity locus and the energy-range climb path. A similar corridor was noted in the energy-modeled study of Ref. 15. The behavior demonstrated by the extremals is fairly transparent. In the optimization process, the optimal tradeoff between the conflicting requirements of a high turn rate and a high energy-rate is established. It is evident that for large heading-to-go, the turn rate is emphasized, and hence control actions are such that flight is on or near the corner-velocity locus. As heading-to-go is decreased, the emphasis shifts toward high energy and range rates, and the control actions are such that the flight is directed generally toward the energy-range climb path.

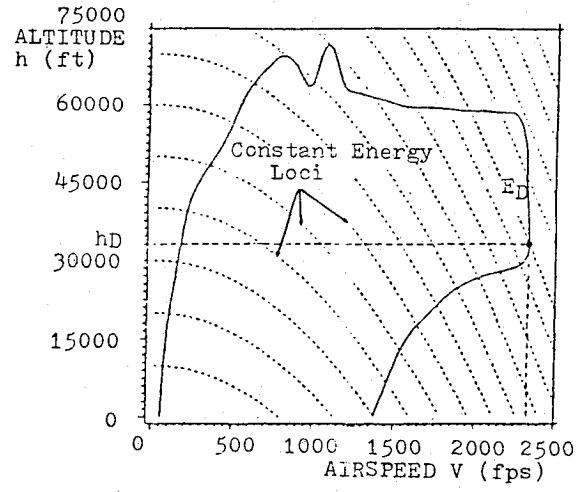

Fig. 1 Steady-state flight envelope and dash-point.

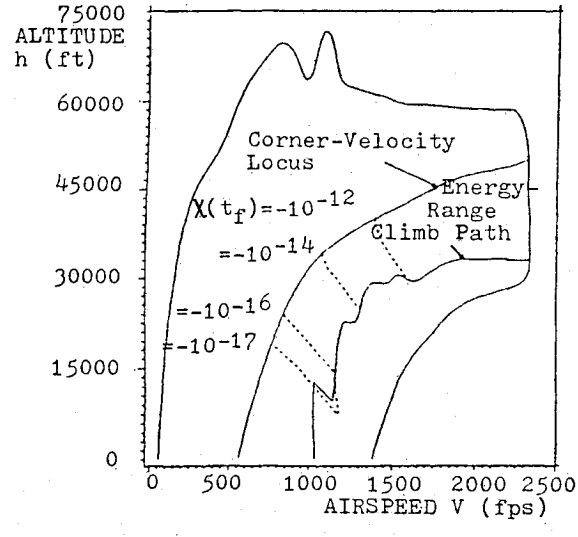

Fig. 2 Energy-state solutions in the (V,*h*)-space.

It is possible to express the family of energy-state solutions in a feedback form: $h^* = h(E,\chi)$, $\mu^* = \mu(E,\chi)$, and $\eta^* = \eta(E,\chi)$. The energy/heading family of energy-state solutions is seemingly an attractive candidate to serve as a "reference family" in a feedback-guidance scheme. Unfortunately, however, the energy-state model exhibits several undesirable features that impair the suitability of this model for such an application. The most unrealistic features in the energy-state model are the instantaneous jumps in altitude occuring sometimes internally as well as at the endpoints (to meet the boundary conditions) and the fact that the approach results in zero flight-path angle approximation.

Singular-perturbation techniques may be used to overcome some of the weaknesses in the energy-state model. Boundary-layer corrections can be used to generate smooth transients from the endpoints to a member of the reference family. However, this is by no means a straightforward procedure. There is currently no rigorous method to identify time-scale separation in nonlinear dynamic systems. In most singular-

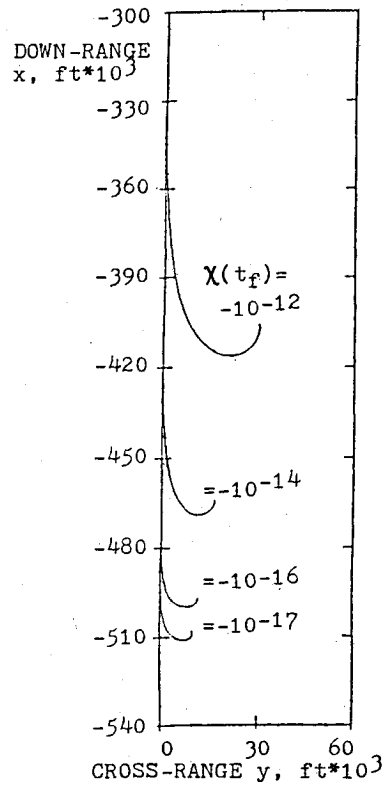

Fig. 3 Ground tracks of energy-state solutions.

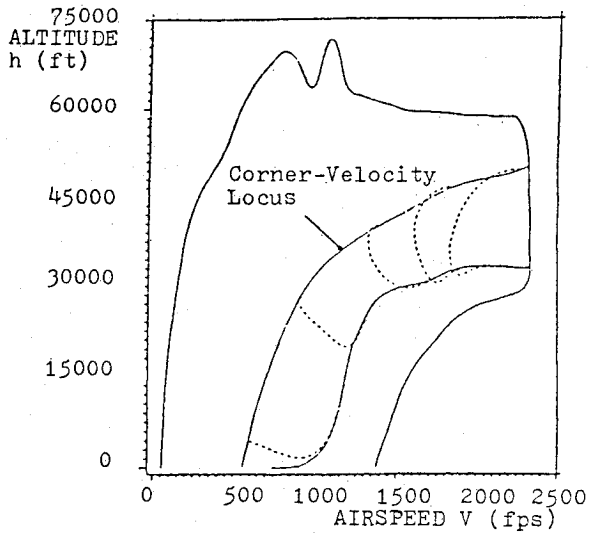

Fig. 4 Point-mass-model state-Euler solutions in the (V,*h*)-space.

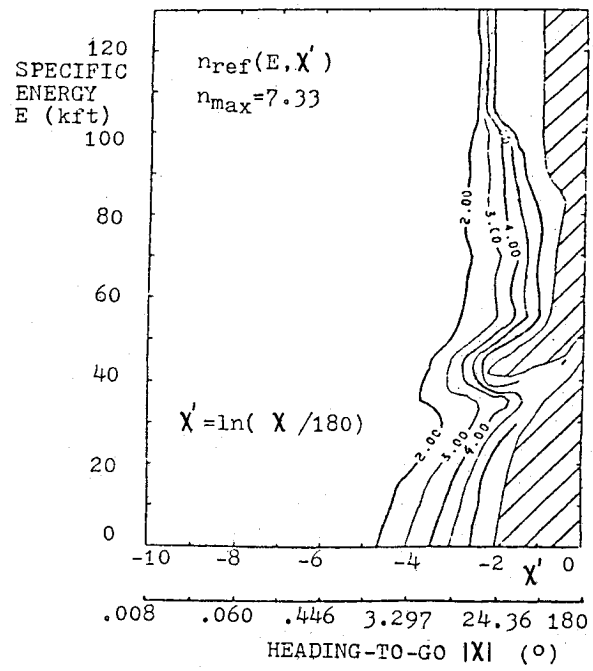

Fig. 5 Feedback control map of n_{ref} (E,χ').

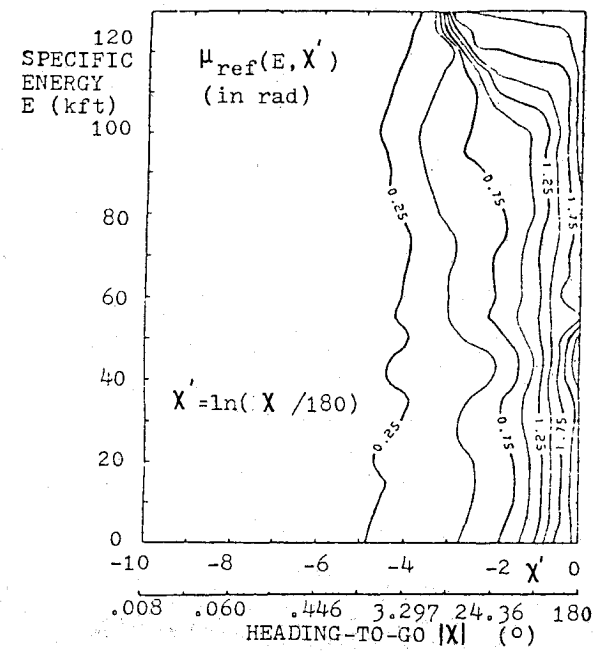

Fig. 6 Feedback control map of μ_{ref} (E,χ').

perturbation analyses, a boundary-layer structure is assumed based on ad hoc time-scale separation judgment.[16] If all dynamical equations are ordered on separate time scales, it may be possible to obtain a closed-form feedback solution.[2,3] However, if altitude and flight-path-angle dynamics are considered on separate time scales, these dynamics are effectively decoupled. It is well-known that altitude and flight-path-angle dynamics are actually highly coupled.[17] On the other hand, if altitude and flight-path-angle dynamics are considered on the same time scale,[1] the boundary-layer solution is not obtainable in feedback form. Internal boundary layers pose even greater problems.[18]

IV. Point-Mass Model

Reference Family

The alternative procedure proposed in Ref. 9, which avoids many complications but is still simple enough to lend itself to onboard implementation, is now developed for the three-dimensional intercept mission. In the proposed scheme, a hierarchical structure similar to that of the energy-state model is assumed: the trajectories of an energy/heading family (reference family) funnel into a steady-state cruise-dash, and the trajectories of an altitude/path-angle family (boundary-layer transients) funnel into individual members of the energy/heading family.

Rather than using energy-state solutions to build up the reference family (as in the singular-perturbation approach), the present approach uses a family of point-mass-model state-Euler solutions. The energy-state solutions are used to select the initial conditions for the individual point-mass-model trajectories that form the reference family. Since we

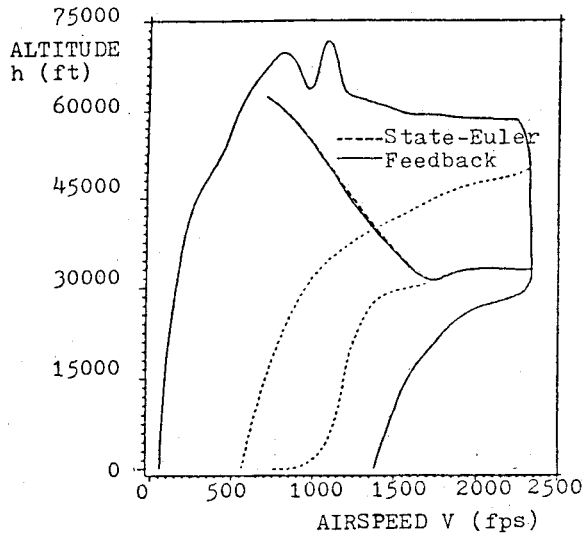

Fig. 7 Solution in the (V,*h*)-space for example intercept mission.

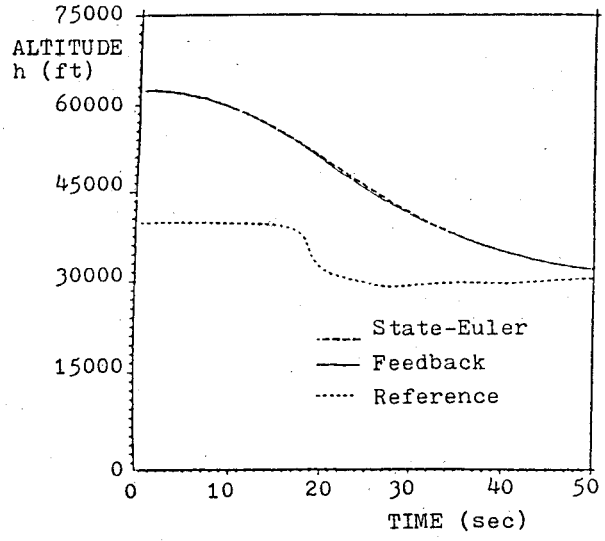

Fig. 8 Altitude history for example intercept mission.

desire a reference family extending over the widest range of energy and heading possible, the initial heading-to-go for the individual trajectories is selected as 180 deg (this choice provides us a complete 360-deg heading range due to symmetry). The energy-state solutions suggest a zero initial path-angle and an initial altitude on the corner-velocity locus. It should be noted that a different path-angle estimate is produced if a different selection of "slow" and "fast" variables is used in the energy-state analysis. This is shown in Ref. 19, where a transformation of state variables is proposed with the objective of enhancing time-scale separation. Investigations along these lines are of future interest. Initial range-to-go is selected sufficiently large to allow an asymptotic approach of the equilibrium point for each individual member of the family (700 kft). Since we assume the behavior of the point-mass-model trajectories to be similar to that of the energy-state model, we anticipate heading to asymptotically reach zero, and, with the prejudice of foresight, Eq. (16) is reduced to

$$\lambda_x = -1/V_D \tag{19}$$

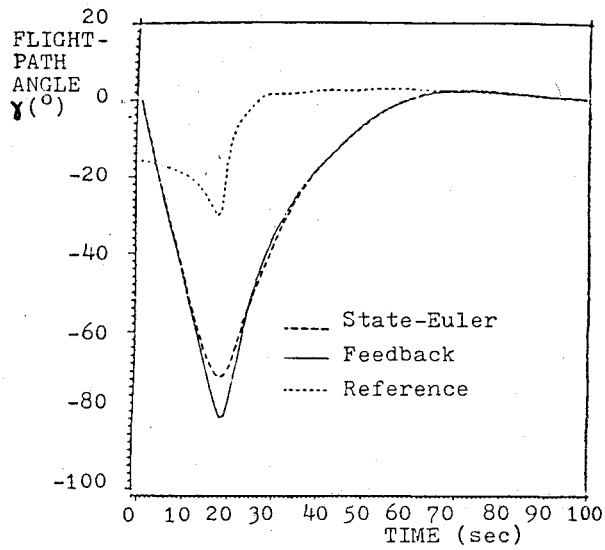

Fig. 9 Flight-path angle history for example intercept mission.

Numerical Solution of the TPBVP

Using the results of Eqs. (14) and (19), the TPBVP is reduced to a set of 10 differential equations, nine of which are given by Eqs. (1) and (12c–12e). A tenth differential equation results if the parameter t_f is treated as a state variable:

$$\dot{t}_f = 0 \tag{20}$$

The 10 boundary conditions needed to solve these equations are given by Eqs. (10) and (11).

As mentioned earlier, state-Euler solutions are generated using a multiple-shooting algorithm (MSA). The main advantage of this method is that numerical-error growth is suppressed by dividing the integration interval into a number of subintervals. Since the state-Euler system associated with the point-mass model is highly unstable, this is an important feature. A similar advantage can be attributed to the special form in which the TPBVP is formulated. Despite the fact that zero final heading is desired, this parameter is not formally prescribed in the present effort. The special form in which the problem is formulated allows the desired final heading to be reached asymptotically. If we do specify final heading, the initial value of the heading adjoint must be iterated upon. The state-Euler system is extremely sensitive to this parameter, and severe stability problems result.[11] In the present approach, the initial crossrange is iterated upon, and no serious stability problems have been experienced. One of the most important contributions of the present research effort is that the heading adjoint, a major source of stability problems, has been eliminated from the problem by paying careful attention to such aspects as the location and orientation of the reference frame, the stipulation of boundary conditions, the closed form integration of some of the adjoint equations, and the use of first integrals.

Some of the point-mass trajectories of the reference family are shown in Fig. 4. The energy management features observed earlier in the energy-state model are validated by these point-mass model results.

V. The Feedback Solution

Guidance Scheme

The next step is to generate a near-optimal guidance law that will transfer the interceptor to the vicinity of the reference family. A closed-loop controller, based on the linear feedback of altitude and path-angle errors (where error is defined as the difference between the actual and the

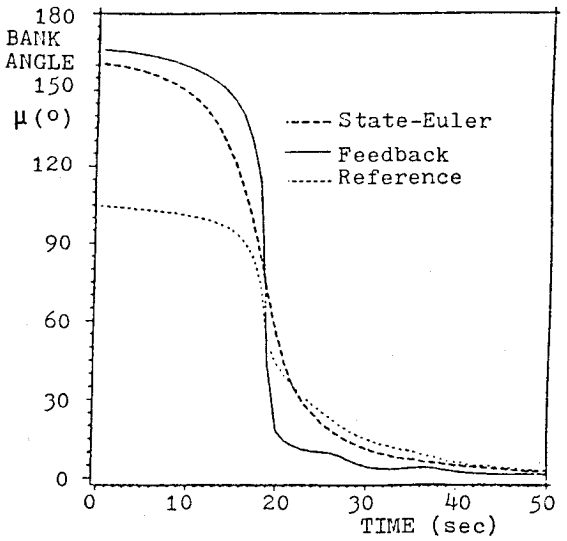

Fig. 10 Bank-angle history for example intercept mission.

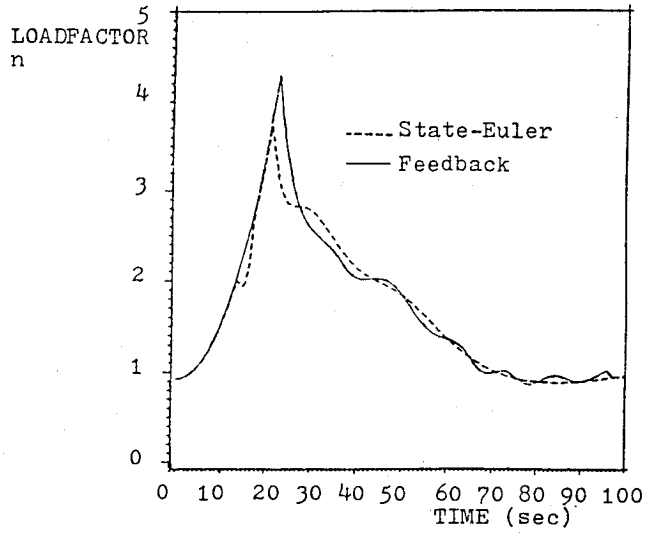

Fig. 11 Load-factor history for example intercept mission.

nominal value), is designed along the lines contemplated in Ref. 9. The resulting feedback laws are

$$n_{fb} = n_{\text{ref}}(E,\chi') + \frac{\partial n}{\partial h}(E,\chi')[h-h_{\text{ref}}(E,\chi')] + \frac{\partial n}{\partial \gamma}(E,\chi')[\gamma-\gamma_{\text{ref}}(E,\chi')] \tag{21a}$$

$$\mu_{fb} = \mu_{\text{ref}}(E,\chi') + \frac{\partial \mu}{\partial h}(E,\chi')[h-h_{\text{ref}}(E,\chi')] + \frac{\partial \mu}{\partial \gamma}(E,\chi')[\gamma-\gamma_{\text{ref}}(E,\chi')] \tag{21b}$$

Evidently n_{fb} is subjected to the constraints of Eqs. (8) and (9). The sign of μ_{fb} is selected such that $|\chi|$ decreases in time ($-\pi \le \chi \le \pi$). The reference variables, i.e., altitude, flight-path angle, the controls, and the feedback gains, are functions of two variables:

$$E, \quad \chi' = \ell n(|\chi|/\pi) \tag{22}$$

These eight functions, represented via spline lattices, are to be stored for onboard use. The particular choice of the nondimensional variable χ' accounts for the exponential character of the heading transient and ensures that the reference variables can be accurately represented by the spline lattices over the entire range of energy and heading.

It is noted that the control laws of Eq. (21) are independent of the crossrange y. The execution of these laws during an engagement may therefore actually cause the interceptor to fly parallel to rather than behind the target in the dash phase of the mission. Assuming that the initial crossrange is small compared to the total range-to-go, a simple offset correction can be devised to overcome this problem. The offset correction is obtained by adding a correction term to the measured value of the heading angle:

$$\Delta\chi = \arctan[y/(x_f - x)] \tag{23}$$

In Figs. 5 and 6, the reference feedback control maps are shown. The regions where the load factor is constrained [by either Eq. (8) or Eq. (9)] are cross-hatched in Fig. 5. The gap separating the two constrained-control areas has been the subject of speculation. In this region, the aircraft dives through the transonic region while executing a rather hard turn. It is conjectured that the load factor is slightly reduced below its constrained level in order to temper the effect of the transonic drag rise.

Feedback Gains

The feedback gains in the guidance scheme are obtained in the difference-quotient approximation as the average of the forward and backward differences. To this end, for each initial condition, calculations are redone with small perturbations from the reference values in altitude and flight-path angle. The feedback gains are evaluated along the reference trajectories by successively treating intermediate points as "new" initial conditions. In order to compute the feedback gains accurately, highly accurate state-Euler solutions are needed.[10,11] The MSA proved to be an extremely powerful tool in this respect.

VI. Numerical Examples

The guidance scheme was tested in digital simulation runs using a point-mass vehicle model. The range of validity of the feedback laws was examined by comparing approximate feedback solutions to open-loop state-Euler solutions for a wide variety of initial conditions. It was found that the feedback laws perform more than satisfactorily, even for extreme deviations from the nominal state. To illustrate this, a numerical example is presented. The initial conditions for this example are

$$E_o = 75000 \text{ ft} \qquad \chi_o = -150 \text{ deg}$$

$$h_o = 62500 \text{ ft} \qquad \gamma_o = 0 \text{ deg}$$

$$x_f - x_o = 700 \text{ kft}$$

The results are shown in Figs. 7–11. The correspondence between the open-loop optimal and approximate feedback solutions is remarkably close. This particular example shows that even for a deviation of altitude from its nominal value in excess of 20,000 ft, an extremely accurate solution can be achieved.

In all, more than a hundred simulation runs were made.[20] All examples examined (with $-45 \le \gamma_o \le 45$ deg) had an accuracy in terminal payoff of 1% or better.

VII. Concluding Remarks

An automatic guidance scheme for a three-dimensional aircraft intercept mission has been developed. The scheme employs state-Euler solutions for a point-mass model but makes use of singular-perturbation ideas in terms of a hierarchical trajectory-family structure. Indeed, the turn-climb schedules that emerge, fair gracefully into a cruise-dash. Numerical examples revealed that, despite their linear nature, the feedback laws perform accurately even for large departures from the nominal state. Although a substantial numerical effort is required for the synthesis of the feedback laws, the actual onboard execution of the feedback laws is rather simple. In eventual onboard real-time implementation of the scheme contemplated, first-order corrections for weight variation, off-nominal ambient temperature, and winds-aloft will be required. On the indication of the results presented herein, the concept appears to hold promise for extension to other mission performance criteria, such as a weighted combination of time and fuel consumed.

Acknowledgments

This research was supported by NASA Langley Research Center, Dr. Christopher Gracey serving as NASA Technical Officer. Assistance by Dr. Klaus Well of DFVLR with the program BOUNDSOL is gratefully acknowledged.

References

[1]Kelley, H.J., "Aircraft Maneuver Optimization by Reduced-Order Approximation," *Control and Dynamic Systems,* Vol. 10, edited by C.T. Leondes, Academic Press, 1973, pp. 131–178.

[2]Shinar, J., Farber, N., and Negrin, M., "A Three-Dimensional Air Combat Game Analysis by Forced Singular Perturbations," AIAA Paper 82-1327, 1982.

[3]Calise, A.J., "Singular Perturbation Techniques for On-Line Optimal Flight Path Control," *Journal of Guidance and Control,* Vol. 3, July-Aug. 1981, pp. 398–405.

[4]Kelley, H.J., "Guidance Theory and Extremal Fields," *IRE Transactions on Automatic Control,* Vol. 7, 1962, pp. 75–82.

[5]Kelley, H.J., "An Optimal Guidance Approximation Theory," *IEEE Transactions on Automatic Control,* Vol. 9, 1964, pp. 375–380.

[6]Breakwell, J.V., Speyer, J.L., and Bryson, A.E., "Optimization and Control of Nonlinear Systems using the Second Variation," *SIAM Control,* Vol. 1, 1963, pp. 193–223.

[7]Rajan, N. and Ardema, M.D., "Computations of Feedback Strategies for Interception in a Horizontal Plane," AIAA Paper 83-0281, 1983.

[8]Rajan, N. and Ardema, M.D., "Interception in Three Dimensions: An Energy Formulation," *Journal of Guidance and Control,* Vol. 8, 1985, pp. 23–30.

[9]Kelley, H.J. and Well, K., "An Approach to Intercept On-Board Calculations," *Proceedings of the American Control Conference,* San Francisco, CA, June 22–24, 1983.

[10]Weston, A.R., Cliff, E.M., and Kelley, H.J., "On-Board Near-Optimal Climb-Dash Energy Management," *Journal of Guidance and Control,* Vol. 8, 1985, pp. 320–324.

[11]Weston, A.R., "On-Board Near-Optimal Climb-Dash Energy Management," Ph.D. Dissertation, Department of Aerospace and Ocean Engineering, Virginia Polytechnic Institute and State University, Blacksburg, VA, 1982.

[12]Vinh, N.X., "Optimal Trajectories in Atmospheric Flight," Elsevier, Amsterdam, 1981.

[13]Bulirsch, R., "Die Mehrzielmethods zur numerischen Losung von nichtlinearen Randwertproblemen und Aufgaben der optimalen Steuerung," *Lehrgang Flugbahnoptimierung Carl-Cranz-Gesellschaft e.V.,* Oct. 1971.

[14]Schultz, R. and Zagalsky, N.R., "Aircraft Performance Optimization," *Journal of Aircraft,* Vol. 9, Feb. 1972, pp. 108–114.

[15]Boyd, J.R., Christie, T.P., and Drabant, R.E., "Max Maneuver Concept," briefing notes, USAF Armament Laboratory, Elgin AFB, Aug. 1971.

[16]Ardema, M.D. and Rajan, N., "Separation of Time Scales in Aircraft Trajectory Optimization," *Journal of Guidance and Control,* Vol. 8, 1985, pp. 275–278.

[17]Kelley, H.J., "Comments on 'A New Boundary-Layer-Matching Procedure for Singularly Perturbed Systems'," *IEEE Transactions on Automatic Control,* Vol. AC-23, June 1978.

[18]Weston, A.R., Cliff, E.M., and Kelley, H.J., "Altitude Transitions in Energy Climbs," *Automatica,* Vol. 19, 1983, pp. 199–202.

[19]Kelley, H.J., Cliff, E.M., and Weston, A.R., "Energy-State Revisited," *Optimal Control Applications and Methods,* Vol. 7, April 1986.

[20]Visser, H.G., "Energy Management of Three-Dimensional Minimum-Time Intercept," Ph.D. Dissertation, Department of Aerospace and Ocean Engineering, Virginia Polytechnic Institute and State University, Blacksburg, VA, 1985.